Solid-State NMR and Hydrogen-Deuterium Exchange in a Bilayer-Solubilized Peptide: Structural and Mechanistic Implications

M. Cotten,*# R. Fu,* and T. A. Cross*#§

*Center for Interdisciplinary Magnetic Resonance at the National High Magnetic Field Laboratory, #Department of Chemistry, and §Institute of Molecular Biophysics, Florida State University, Tallahassee, Florida 32310 USA

ABSTRACT Hydrogen-deuterium exchange has been monitored by solid-state NMR to investigate the structure of gramicidin M in a lipid bilayer and to investigate the mechanisms for polypeptide insertion into a lipid bilayer. Through exchange it is possible to observe ^{15}N-^{2}H dipolar interactions in oriented samples that yield precise structural constraints. In separate experiments the pulse sequence SFAM was used to measure dipolar distances in this structure, showing that the dimer is antiparallel. The combined use of orientational and distance constraints is shown to be a powerful structural approach. By monitoring the hydrogen-deuterium exchange at different stages in the insertion of peptides into a bilayer environment it is shown that dimeric gramicidin is inserted into the bilayer intact, i.e., without separating into monomer units. The exchange mechanism is investigated for various sites and support for a relayed imidic acid mechanism is presented. Both acid and base catalyzed mechanisms may be operable. The nonexchangeable sites clearly define a central core to which water is inaccessible or hydroxide or hydronium ion is not even momentarily stable. This provides strong evidence that this is a nonconducting state.

INTRODUCTION

A strategy to understand how water and protic solvents interact with a protein and affect protein structure, dynamics, and ultimately function is to study hydrogen-deuterium exchange of amide protons within a protein. The polypeptide, gramicidin M (gM), is a variant of gramicidin A (gA) in which all tryptophan residues have been replaced by phenylalanine. Gramicidin A and M form a variety of well defined structures in organic solvents and lipid bilayers. Hydrogen-deuterium exchange has been monitored by solid-state NMR of uniformly aligned samples for gM in hydrated lipid bilayers. This has led to knowledge of this peptide structural fold, water accessibility, exchange mechanisms, and cation conductance potential for this structure.

Gramicidin A, a major synthetic product of *Bacillus brevis*, is a 15-amino-acid polypeptide. The alternating D and L amino acid sequence induces the backbone to adopt a β-strand type of structure that finds stability as dimeric helical conformations in organic solvents. As shown by solution NMR (Abdul-Manan and Hinton, 1994; Arseniev et al., 1986; Pascal and Cross, 1992, 1993) and x-ray crystallography (Langs, 1988; Langs et al., 1991; Wallace and Ravikumar, 1988) various dimeric structures occur differing in handedness, residues per turn (pitch), and relative position of the helices (parallel or antiparallel) that are dependent on the solvent polarity. In lipid bilayers, the polypeptide forms a monovalent cation-selective channel which has been solved at high resolution using solid-state NMR (Ketchem et al., 1993, 1996). It features an amino terminal-to-amino terminal hydrogen-bonded single-stranded dimer with each monomer folding into a right-handed hydrogen-bonded helix of 6.5 residues per turn. In all of the β-strand helical structures the backbone lines a pore; it has a diameter of 4 Å for the channel conformation and is much smaller for the longer double-stranded structures discussed here. This small pore is shown in this report to be incompatible with cation conductance.

It is well accepted that the left-handed antiparallel double-stranded structure adopted by gA in benzene/ethanol, used to cosolubilize peptide and lipid before bilayer formation, converts readily to the channel state upon insertion in the bilayer. Under these sample preparation conditions, the double-stranded structures are believed to insert as a double-stranded dimer, and then unscrew to form the single-stranded channel (O'Connell et al., 1990; Zhang et al., 1992) rather than insert as monomers that dock to form the channel. The four tryptophan side chains which have been widely studied for their role in defining a favorable fold within a specific environment and in channel function may also have a role in the conversion process. Recently, it was shown that gM is double-stranded in the bilayer (Salom et al., 1995), suggesting that the indoles are fundamentally important for the conversion of the double helices to single-stranded helices (Cotten et al., 1997). To gain some insights about the speculation that gA inserts as a double-stranded dimer that converts within the bilayer, we have used here the gM dimer as a model for the early intermediate state of gA during insertion into the bilayers before conversion to the channel state. The question of whether or not the double-stranded structure unfolds in the time between organic solvent cosolubilization and bilayer formation is also addressed.

Received for publication 9 July 1998 and in final form 10 November 1998.

Address reprint requests to Dr. Timothy A. Cross, National High Magnetic Field Laboratory, Florida State University, 1800 E. Paul Dirac Drive, Tallahassee, FL 32306-4005. Tel.: 850-644-0917; Fax: 850-644-1366; E-mail: cross@magnet.fsu.edu.

0006-3495/99/03/1179/11 $2.00

As early as 1955, Linderstrøm-Lang (1955) suggested that amide proton exchange might be used to derive secondary structure in proteins, but this goal has not yet been realized. However, several findings support this hypothesis: 1) the participation of amide protons in secondary structure is correlated with their protection against exchange, and tertiary structure also affects the pattern of protection (Englander and Kallenbach, 1984; Rohl and Baldwin, 1994; Wagner, 1983; Wagner and Wüthrich, 1982; Woodward et al., 1982); 2) since hydrogen-bonds provide protection against exchange, their breakage is a condition for exchange to occur (Englander et al., 1972). Various models for exchange mechanisms, which can be base- or acid-catalyzed, have been widely discussed (Eriksson et al., 1995). This is an important issue because the interpretation of kinetic results is dependent on the mechanisms of exchange, which themselves depend on the stability of the protein in a given environment. Ultimately, this suggests that it is too complex to identify either a secondary structure from exchange results or to deduce the exchange mechanism(s) taking place from the secondary structure alone. Clearly, a meaningful interpretation of the exchange results in terms of structure and dynamics has to be obtained in light of the underlying physical mechanisms. The relayed imidic acid exchange mechanism reviewed by Eriksson et al. (1995) was introduced very early for its relevance in energy transduction across membranes where proton translocation generates the proton motive force coupled to electron transport of some membrane proteins (Kayalar, 1979). It has also been at the center of several studies of hydrogen-deuterium exchange of proteins in solution, starting with Tüchsen and Woodward (1985) and has successfully been used to explain experimental observations that other mechanisms could not. However, arguments have been raised against this mechanism (Perrin, 1994) and the debate continues. Here, amide exchange in the backbone of gM has led to support for the relayed imidic exchange mechanisms necessitated by the hydrophobic membrane environment.

Solid-state NMR spectra of single-site ^{15}N labeled gM inserted in uniformly hydrated lipid bilayers of DMPC were used to structurally characterize the peptides and study the hydrogen-deuterium exchange of the amide protons through exposure to deuterated protic solvents. The structure has been characterized using orientational constraints derived from ^{15}N chemical shifts and ^{15}N-^{1}H and ^{15}N-^{2}H dipolar interactions that are orientationally dependent in the anisotropic lipid bilayer environment. The large data set for 11 of 15 amino acid residues complements the initial structural data of Cotten et al. (1997) and confirms that the structure is double-stranded and left-handed. Distance measurements in samples undergoing considerable motional averaging have been obtained here using a new approach (Fu et al., 1997) for observing solid-state NMR-derived distances, SFAM, for Simultaneous Frequency and Amplitude Modulation. This dipolar interaction-based approach has shown that the dimer is antiparallel, identical to the solution-state conformation. The extent of exchange assessed from relative peak intensities in the ^{15}N-^{2}H dipolar coupled chemical shift spectra has been used to define the water accessibility profile of the double-stranded dimer within a bilayer.

MATERIALS AND METHODS

Gramicidin M was synthesized by solid phase peptide synthesis using Fmoc (9 fluorenylmethoxycarbonyl) chemistry on an Applied Biosystems model 430A peptide synthesizer. Isotopically labeled amino acids were purchased from Cambridge Isotope Laboratories (Woburn, MA) and the blocking chemistry was performed in our lab. Details of the synthesis and blocking chemistry have been described previously (Fields et al., 1988, 1989).

Once cleaved from the solid phase support, the peptides were characterized and the purity assessed. Crude gM was purified by recrystallization at room temperature after dissolving the peptide at 55°C in HPLC-grade MeOH. The protocol for characterization by HPLC, mass spectroscopy and solution NMR, has been previously described (Cotten et al., 1997).

Oriented samples for solid-state NMR were prepared by codissolving gA or gM and dimyristoylphosphatidylcholine (DMPC) in a 1:8 molar ratio in 95/5 (v/v) benzene/ethanol solution. After a freeze-thaw cycle the solution, while still cool, was spread on glass coverslips. Partial evaporation of the solvents was allowed to occur at room temperature. The samples were then dried overnight under vacuum and stacked in a square glass tube before adding 50% HPLC-grade water (by total sample dry weight). The tubes were then sealed and incubated at 45°C for a minimum of two weeks until the samples became transparent, uniformly hydrated, and oriented such that the bilayers were parallel to the glass slides. Sample pH has been shown in similar preparations to be approximately neutral (Huo et al., 1996).

Deuterium exchange of amide protons was performed by opening a previously hydrated sample and exposing the sample to a saturated D_2O atmosphere at 45°C for a minimum of 4 days and, if exchange did not occur after this lapse of time, for at least 20 days in a closed container. The attributes "partially exchangeable" (Val_7) and "nonexchangeable" refer to the extent of exchange observed after this exposure time of ~20 days. If a significant weight loss occurred during the incubation, D_2O was added to compensate. The samples were then sealed and further incubated.

Solid-state NMR spectra were acquired using a spectrometer built around a Chemagnetics data acquisition system and an Oxford Instruments 400/89 magnet. The ^{15}N resonant frequency was 40.58 MHz and the spectra were recorded using cross-polarization (5-μs 90° pulse, 1 ms contact time, 7 s recycle delay) and ^{1}H dipolar decoupling. ^{15}N-^{1}H separated local field (SLF) experiments were recorded with a second dimension dwell time of 20 μs and typically 1000 acquisitions for each of the 16 t_2 values. The ^{15}N spectra were referenced to a saturated solution of $^{15}NH_4NO_3$.

Distance measurements in hydrated powder (unoriented) samples were implemented by using the recently developed simultaneous frequency and amplitude modulation (SFAM) dipolar recoupling scheme (Fu et al., 1997) on a Bruker DMX 300 spectrometer with resonance frequencies of 30 MHz for ^{15}N and 75 MHz for ^{13}C. A 2 kHz sample spinning rate about the magic angle was used in order to completely suppress the chemical shift anisotropy. After enhancement by cross-polarization, the ^{13}C magnetization evolves during two intervals separated by a 180° pulse, and then the ^{13}C signals were recorded at the echo time. A 180° ^{15}N pulse was also applied between the intervals. When the SFAM irradiations are applied to the ^{15}N spins during the intervals, the observed ^{13}C signals dephase due to the recovered ^{13}C-^{15}N dipolar coupling. The parameters used for SFAM in our experiments were an ^{15}N modulation frequency of 2 kHz (equal to the spinning speed), depth of the frequency modulation 30 kHz, and an RF amplitude of 25 kHz. The 180° pulsewidth was 16.8 μs for both ^{15}N and ^{13}C. A recycle delay of 4 s was used and conventional CW proton decoupling was applied throughout the evolution and observation of the ^{13}C magnetization.

The spectral data were processed using Felix software (Biosym Technologies, San Diego, CA). The computational work was performed on a

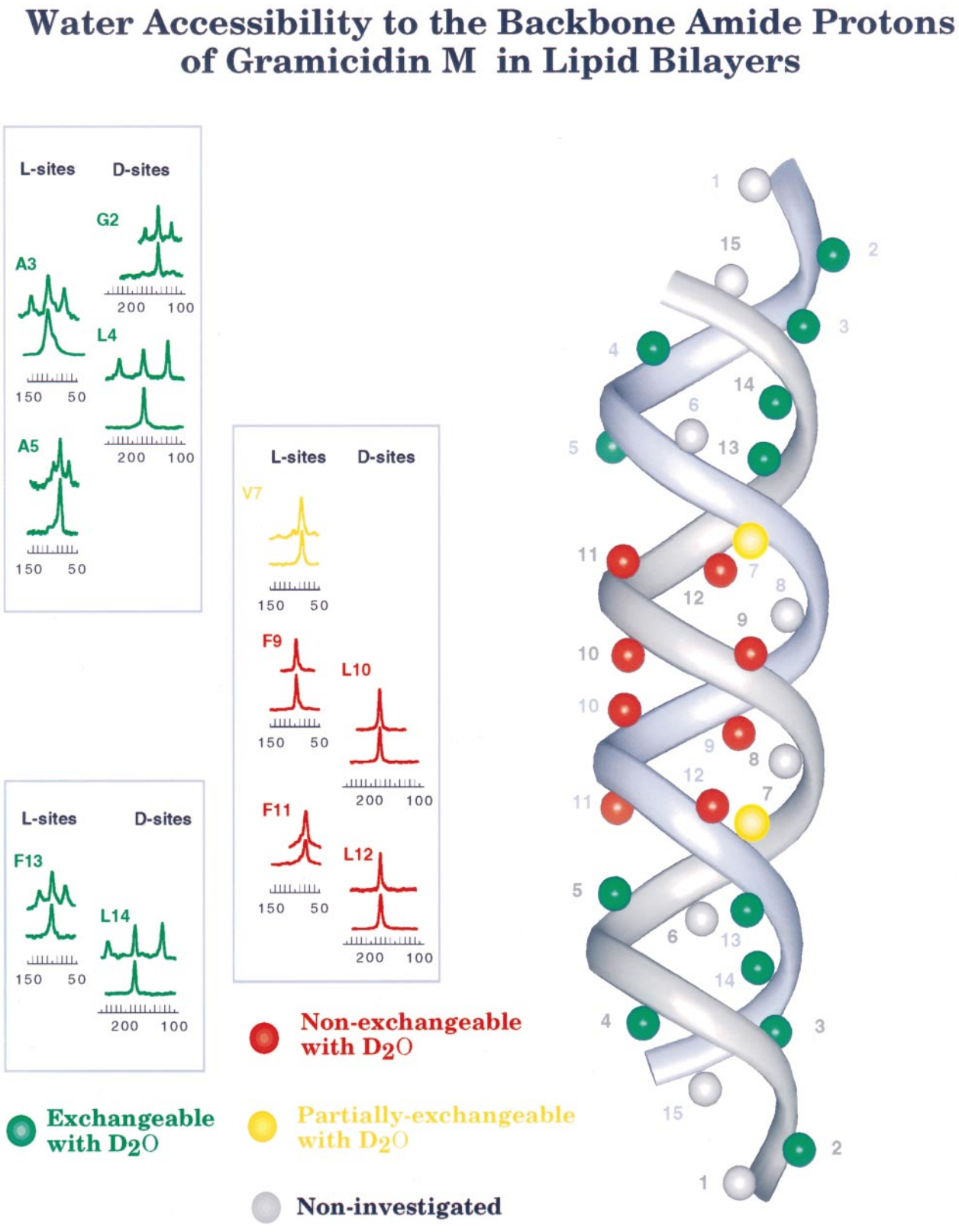

FIGURE 1 On the left side of the figure, ^{15}N chemical shifts (*bottom spectrum*), and ^{15}N-^{2}H dipolar interactions (*top spectrum*) are displayed for each of the 11 ^{15}N-single-site-labeled gM samples prepared in oriented, hydrated DMPC bilayers. Deuterium exchange of amides was performed by exposing a previously hydrated sample to D_2O for at least four days. Green, yellow, and red color are used for exchangeable, partially, and nonexchangeable sites, respectively. On the right side of the figure, the propensity for deuterium exchange of the 11 sites has been indicated on the antiparallel, left-handed, and double-stranded structure which is highly stabilized by 28 intermolecular backbone hydrogen bonds. The exchangeable sites (*green*) are located at both ends of the dimer. The nonexchangeable sites (*red*) are concentrated in the middle of the peptide, which suggests that the central part of the dimer is too narrow to accommodate water. The two monomers are distinguished by gray and blue. The spectra at the left are aligned with the residue positions for the blue monomer.

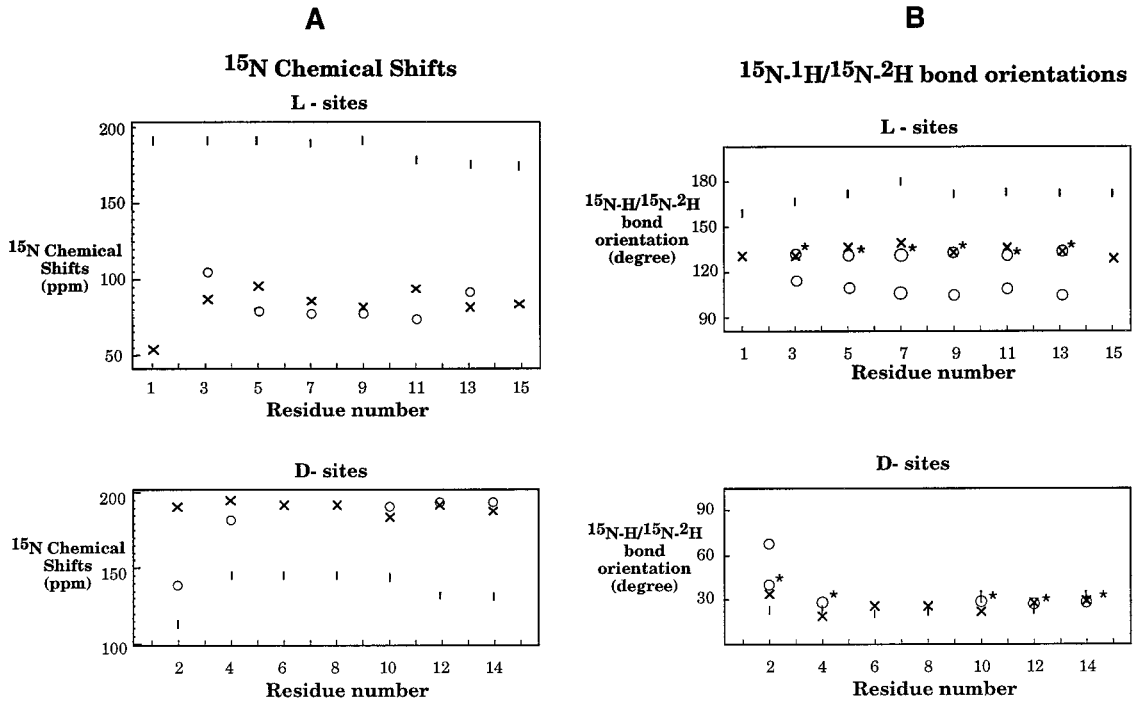

FIGURE 2 (*A*) The observed values of the ^{15}N chemical shifts of gM (*circles*) from Fig. 1 are plotted as a function of residue number, and compared to two structures: the observed CS of the gA channel state (*vertical bars*, Ketchem et al., 1993) and predicted CS values for the species 3 structure (*crosses*, Pascal et al., 1994). (*B*) Same as in (*A*) but for the ^{15}N-^{2}H bond orientations of gM (*circles*), the gA channel state (*vertical bars*, Ketchem et al., 1993) and species 3 structure (*crosses*, Pascal et al., 1994). Due to the magnitude of the dipolar interactions, two ^{15}N-^{2}H bond orientations are possible based on the dipolar data for the L-sites. *, One set of orientations follows the same pattern as for species 3.

Silicon Graphics Indigo 2 Extreme work station. The simulations for the distance measurements were performed on the GAMMA platform (Smith et al., 1994).

RESULTS

On the left side of Fig. 1, the spectra summarize the results for single-site ^{15}N-labeled gM inserted into lipid bilayers. For each of 11 amino acids, a pair of spectra are shown (positions 1, 6, 8, and 15 have not been investigated). The bottom spectrum of each pair represents the ^{15}N chemical shifts (CS) from fully protonated samples. The resonances for D and L amino acid residues alternate between ~180 and 85 ppm, respectively. This is in sharp contrast with the pattern observed for gA in the channel conformation: ~135 and 198 ppm for D and L sites, respectively (Nicholson and Cross, 1989). The graph in Fig. 2 *A* plots these ^{15}N chemical shifts versus residue number and compares them with the chemical shifts experimentally determined for the gA channel state and predicted for the left-handed antiparallel double-stranded structure of gA in organic solvents. These latter chemical shifts were calculated using the coordinates of the structure published by Pascal and Cross (1992). The ^{15}N chemical shifts of the membrane-spanning gM structure correlate very well with the calculated chemical shifts from species 3.

The top spectra on the left side of Fig. 1 were recorded after exposure of the samples (used for the bottom spectra) to D_2O. Exchangeable sites give rise to a dipolar splitting in the ^{15}N chemical shift spectrum resulting in a triplet which is caused by the dipolar interaction between a spin-½ site (^{15}N) and a spin-1 site (^{2}H). The triplet centered on the ^{15}N chemical shift frequency has a nominal 1:1:1 intensity for fully exchanged sites. The outer resonances may have a smaller intensity than the center peak, suggesting either incomplete exchange and therefore poor accessibility of the site to water, or one of the resonances may be broader than the others and hence of lower intensity due to relaxation effects.

From the observed triplets, the magnitude of the ^{15}N-^{2}H dipolar interactions has been extracted and the ^{15}N-^{2}H bond orientations calculated with respect to B_o and the helical axis of the dimer (see Cotten et al., 1997; Tian et al., 1996 for calculations). For nonexchangeable sites, SLF experiments were used to obtain the ^{15}N-^{1}H bond orientations. We have compared the ^{15}N-^{1}H (observed before exposure to D_2O) and ^{15}N-^{2}H (after exposure to D_2O) bond orientations for position 4 and obtained the same values. This has confirmed that the two methods are consistent and that the bond orientation is not perturbed by deuteration. In Fig. 2 *B*, a graphic representation of ^{15}N-^{1}H- or ^{15}N-^{2}H-derived bond orientations versus residue number is presented for the L and D residues. These data are compared, as in Fig. 2 *A*, with the N-H bond orientations from the single-stranded gA channel state and from species 3. All three sets of N-H bond

orientations are close to 30° for the D sites. However, the L sites show that the channel state has orientations close to 180°, whereas these orientations are 130° for the membrane-spanning gM and species 3 structures. Therefore, L sites permit differentiation between single- and double-stranded structures and as shown previously (Cotten et al., 1997) these data distinguish between left- and right-handed structures. While it is shown here that gM is left-handed and double-stranded, the parallel versus antiparallel question has not been resolved with orientation constraints. However, distance measurements reported here make this characterization possible.

The SFAM method for measuring heteronuclear dipolar interactions for distance constraints was used here for its sensitivity to the small dipolar interactions. The side views of parallel and antiparallel structures are represented in Fig. 3 using species 3 and species 4 structures, respectively, as models. Since the antiparallel structure was expected, the position of the isotopic labels was chosen to span a hydrogen-bonded pair of peptide planes in species 3 and not in species 4. Intermonomer hydrogen-bonded ^{13}C carbonyl and amide ^{15}N groups are ~4 Å apart, a reasonable distance for detection by SFAM. As shown in Fig. 3, we have incorporated ^{13}C into the carbonyl of Ala_5 and ^{15}N into the amide nitrogen of Phe_{11}. In the parallel structure this distance would be 10 Å and the $^{15}N/^{13}C$ dipolar interaction would be too small to be detected. Note that in both structures, the intramolecular distance between ^{13}C and ^{15}N is long (>9 Å). Therefore, the residual dipolar interactions arising from this intramolecular interaction can be neglected compared to the targeted $^{13}C/^{15}N$ intermonomer dipolar interactions between sites ~4 Å apart.

In Fig. 4, spectra using several dephasing times of the SFAM pulse sequence applied to gM inserted into hydrated unoriented lipid bilayers are displayed and compared with the ones obtained with no dephasing. The peak at 174 ppm is not affected by the dephasing due to the ^{15}N dipolar interaction, and is therefore assigned to the carbonyl groups

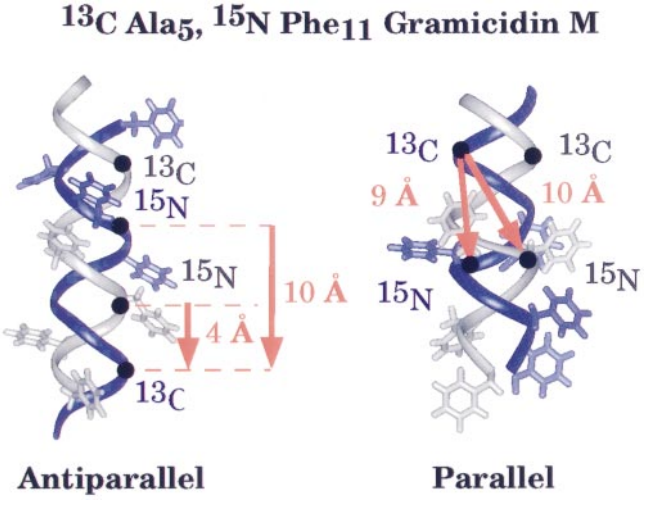

FIGURE 3 Distance measurements for a parallel (species 4), and antiparallel species 3 structure are made based on the incorporation of a ^{13}C in the carbonyl of Ala_5, and a ^{15}N in the amide of Phe_{11}. While the intermonomer distance is ~4 Å in the antiparallel structure, it is ~10 Å in the parallel structure. The intramonomer distances in both structures are too long to give rise to detectable dipolar interactions.

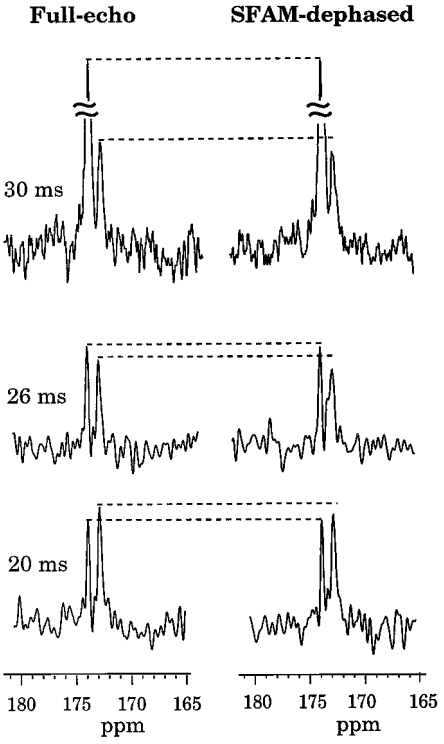

FIGURE 4 A set of SFAM spectra of ^{13}C Ala_5, ^{15}N Phe_{11} gM in unoriented hydrated DMPC bilayers recorded at 315 K (above the phase transition temperature), and using different dephasing durations (*right*) is compared to the full echo set (*left*). The peak at 174 ppm is not affected by dephasing, and is therefore assigned to the carbonyl group of the lipids. The peptide resonance is at 173 ppm, and is modulated by the ^{15}N label.

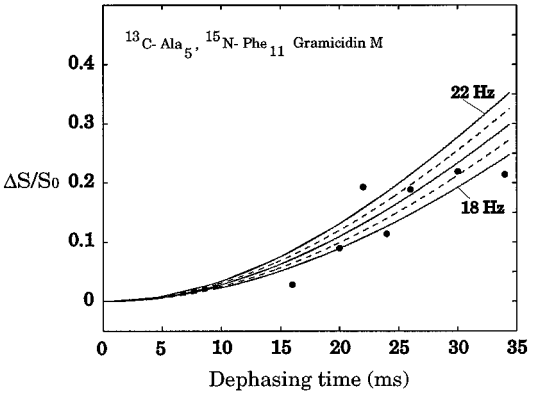

FIGURE 5 The signal intensities of ^{13}C Ala_5, ^{15}N Phe_{11} gM from the spectra in Fig. 4 are used to graph the ratio of SFAM difference (ΔS) to full-echo (S_0) intensity versus dephasing time. The experimental data (*dots*) is compared to plots simulated for dipolar interactions varying from 18 to 22 Hz by increments of 1 Hz. The average dipolar interactions between these labels is 19 ± 3 Hz, corresponding to a motionally averaged distance of 4.5 ± 0.3 Å.

of the lipids. The peptide resonance at 173 ppm is dephased and its intensity is used to generate the graph in Fig. 5. Here, ratios of SFAM difference to full echo intensities are plotted versus dephasing times. The dimer undergoes a global rotation around its helical axis with a correlation time shorter than the frequency scale of the $^{13}C/^{15}N$ dipolar interactions observed here (Lee et al., 1993; North and Cross, 1995). So the comparison of the experimental values with simulated curves for various dipolar interactions allows for the deduction of a motionally averaged dipolar interaction. The effect of the peptide motional averaging on the observed dipolar interaction has been taken into account by including a scaling factor in the distance calculation. The orientation of the intermolecular ^{13}C-^{15}N vector with respect to the axis of molecular motion (the helical axis of the dimer and bilayer normal) has been estimated as 32° from the gramicidin species 3 model, yielding a scaling factor of 0.6. The motionally averaged dipolar interaction obtained from the data in Fig. 6 is 19 ± 3 Hz. The distance calculated taking into account the scaling factor is 4.5 ± 0.3 Å. This is consistent only with the antiparallel gM structure, the same species 3 conformation observed in benzene/ethanol (95%/5%) solvent used for cosolubilizing lipid and peptide in the preparation of the bilayer samples.

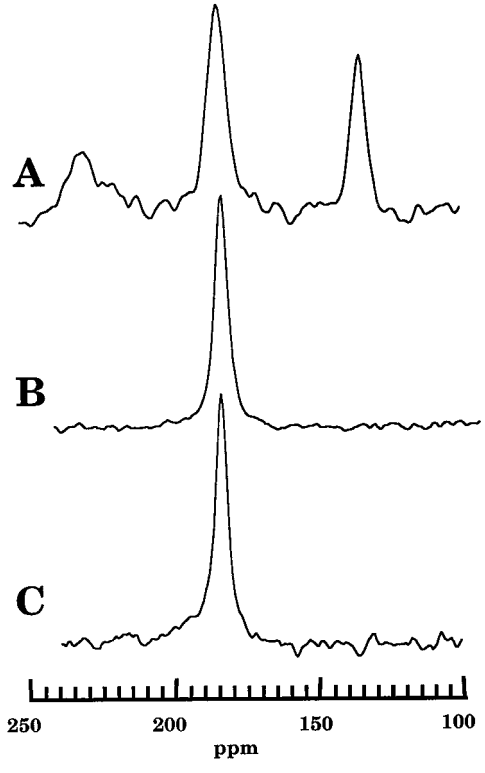

FIGURE 6 Spectra obtained for ^{15}N Leu_{10} gM after exposure to (*A*) recrystallization, cosolubilization, and hydration in deuterated solvents; (*B*) hydration with D_2O of the dry lipid/peptide sample; C) hydration with H_2O of the dry lipid/peptide sample followed by exposure to D_2O. Only in (*A*) is the amide proton exchanged as indicated by the splitting of the ^{15}N resonance to a triplet.

In terms of exchangeability, a qualitative analysis of the ^{15}N-^{2}H dipolar results indicates that the amino acid residues can be classified as follows: 1) exchangeable sites at position 2 through 5 at the amino end and 13 and 14 at the carboxyl end; 2) nonexchangeable sites at position 9 through 12 in the middle portion of the peptide; and 3) position 7 is partially exchanged under the experimental conditions used (20 days or more exposure to D_2O at approximately neutral pH). Positions 1, 6, 8, and 15 have not been investigated. We conclude that the water-accessible ends are separated by a stretch of nonexchangeable sites as illustrated on the right side of Fig. 1.

In the interest of understanding whether the dimer present in organic solvents is the same dimer in the bilayer environment (i.e., the same two monomers) deuterium exchange has been conducted under several conditions using ^{15}N Leu_{10}-labeled gM (Table 1). When the peptide is exposed to D_2O after peptide insertion into the bilayers the ^{15}N-^{1}H is not exchanged (Figs. 1 and 6 *C*). When D_2O is used initially to hydrate the sample to form bilayers, no exchange occurs (Fig. 6 *B*). Only when the peptide is recrystallized and codissolved with the lipids using deuterated solvents (d_4-methanol and d_6-ethanol) does exchange occur (Fig. 6 *A*). Therefore, exposing the peptides to deuterated solvents in an environment where the peptide conformers are known to interconvert (i.e., break and reform hydrogen bonds) is required to achieve exchange for the central sites (Fig. 1, *red*).

DISCUSSION

The orientational and distance constraints for gM in a lipid environment support the left-handed, double-stranded antiparallel structure, previously described as species 3 where it has been shown to exist in numerous organic solvents. The resistance of the Leu_{10} N-H to exchange with solvent water at any time in the reconstitution of the peptide into a bilayer environment from the time when the peptide and lipid were dried from a cosolubilizing organic solvent shows that this N-H is protected from exchange throughout this process. In the cosolubilizing solvent aggregation of the lipid and lipid-peptide does not occur. This suggests that Leu_{10} maintains

TABLE 1 ^{15}N Leu_{10} gM subjected to various experimental conditions to test its protection against hydrogen-deuterium exchange

Experimental Step	Solvent System		
	A	B	C
Recrystallization	MeOD	MeOH	MeOH
Codissolution with lipids	EtOD/Bzn	EtOH/Bzn	EtOH/Bzn
Hydration 1	D_2O	D_2O	H_2O
Hydration 2	N/A	N/A	D_2O
Exchangeable?	YES	NO	NO

A, Recrystallization, cosolubilization, and hydration in deuterated solvents; B, hydration with D_2O of the dry lipid/peptide sample; C, hydration with H_2O of the dry lipid/peptide sample and exposure to D_2O of the oriented sample.

its intermolecular hydrogen bond and that the specific monomers involved in a species 3 dimer, present in the organic solvents, remains intact through the reconstitution into the lipid environment, even during the dry stages of this process. Only when this site is fully exposed to a catalytic solvent (Xu et al., 1996) that induces structural interconversion (e.g., methanol or ethanol) does exchange occur. The distribution of exchangeable sites (Fig. 1, *green*) compared to nonexchangeable sites (*red*) illustrates a nonexchangeable middle portion and exchangeable ends of the peptide. This symmetry is consistent only with the double-stranded type of structure. Potentially, the difference in exchangeability observed for Val_7, Phe_9, and Ala_5 could be due to side chain effects. In a scenario where direct catalysis was operating it would be base catalyzed at neutral pH. Using the coefficients given by Bai et al. (1993, Tables II and III) which take into account the steric and inductive effects of the L-amino acids neighboring a given N-H, the rate constants k_b, for the base-catalyzed exchange reactions in an all L-amino acid gM backbone, have been estimated in Table 2. Since the even-numbered residues are D- amino acids in gM with the exception of Gly_2, the numbers in Table 2 are approximations that ignore this stereochemistry. However, no correlation exists between these values and the exchange data shown here. For instance, Phe_9 is nonexchangeable, but has a k_b that is three times that of the partially exchangeable Val_7 and on the same order as the k_b of the readily exchangeable Leu_4 and Leu_{14}.

In previous studies of gA, also having a species 3 conformation in organic solvents, it was suggested that this peptide inserts initially as a double-stranded structure in the bilayer environment and then rearranges to form the single-stranded channel conformation (O'Connell et al., 1990; Zhang et al., 1992). GM brings evidence to this hypothesis since the double-stranded structure remains intact from the solvent solubilization, through the dry stages of the process, and into the lipid bilayer, thereby providing a model intermediate state for gA along the bilayer insertion pathway, i.e., the species 3 structure in a lipid bilayer environment.

From the species 3 structure of gA determined in organic solvents, it was speculated that if gM formed a similar conformation in a lipid environment, it would represent a nonconducting state because of the pore dimensions (Fig. 7; Cotten et al., 1997). The nonexchangeability of the backbone amide protons in the middle of the membrane spanning structure provides direct evidence that water is not present in the structural pore (Fig. 1) or that if present, it does not exchange with the bulk solvent. When water is present, as in the gA channel conformation, all amide N-H groups exchange in <10 h under these sample conditions. Here, in 20 or more days these amides in the center of this structure do not exchange even within detection limits (Huo et al., 1996). The rate at which D_2O can replace H_2O in the oriented sample has previously been estimated to be 2 h (Huo et al., 1996). When no lipid was present, both Xu et al. (1996, by NMR) and Langs (1988, by x-ray diffraction) failed to find solvent molecules in the species 3 pore, consistent with our findings for the same conformation in the lipid environment. If indeed water is not present in the pore, then this structure cannot be a conducting state because stripping the entire hydration sphere from a cation is energetically too costly for this peptide to provide an adequate compensating solvation environment (Tian and Cross, 1999, in press). However, gM has been shown to conduct cations (Fonseca et al., 1992). Furthermore, the conducting states have a short lifetime, a feature inconsistent with the double-stranded state. Consequently, Heitz et al. (1986), as well as Koeppe and Andersen (1996) concluded that the gM conducting state has a similar backbone structure to gA, i.e., a single-stranded structure. Our solid-state NMR study has the advantage of detecting structures independent of their functionality and shows that the major conformational state of gM at equilibrium is double-stranded ($>95\%$). It could be argued that gM structure is different in samples prepared for conductance studies where DPhPC/decane is frequently used. However, recent structural and conductance studies with a variety of lipids have suggested that the gA structure in DPhPC/decane and the structure in DMPC are very

TABLE 2 Calculated solvent-exposed amide hydrogen exchange, k_b, for an all-L-amino acid gM backbone at neutral pH

Residue	k_b (min^{-1})
Val-1	13
Gly-2	85
Ala-3	93
Leu-4*	17
Ala-5	39
Val-6*	13
Val-7	9
Val-8*	9
Phe-9	26
Leu-10*	19
Phe-11	22
Leu-12*	19
Phe-13	22
Leu-14*	19
Phe-15	22

The coefficients used to take into account the inductive and steric effects from the side chains are from Bai et al., 1993 for L-amino acids (Table II). The k_b reference rate is the one given in Table III in the same reference for PDLA under normal low salt concentrations.
*These residues are D-amino acids in gM.

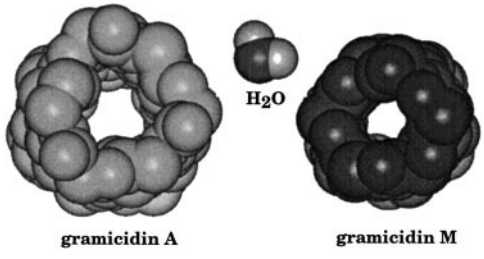

FIGURE 7 End views of single-stranded gA channel (*left*), and double-stranded gM pore (*right*) are displayed using the same scale, and van der Waals spheres. For comparison a water molecule is shown.

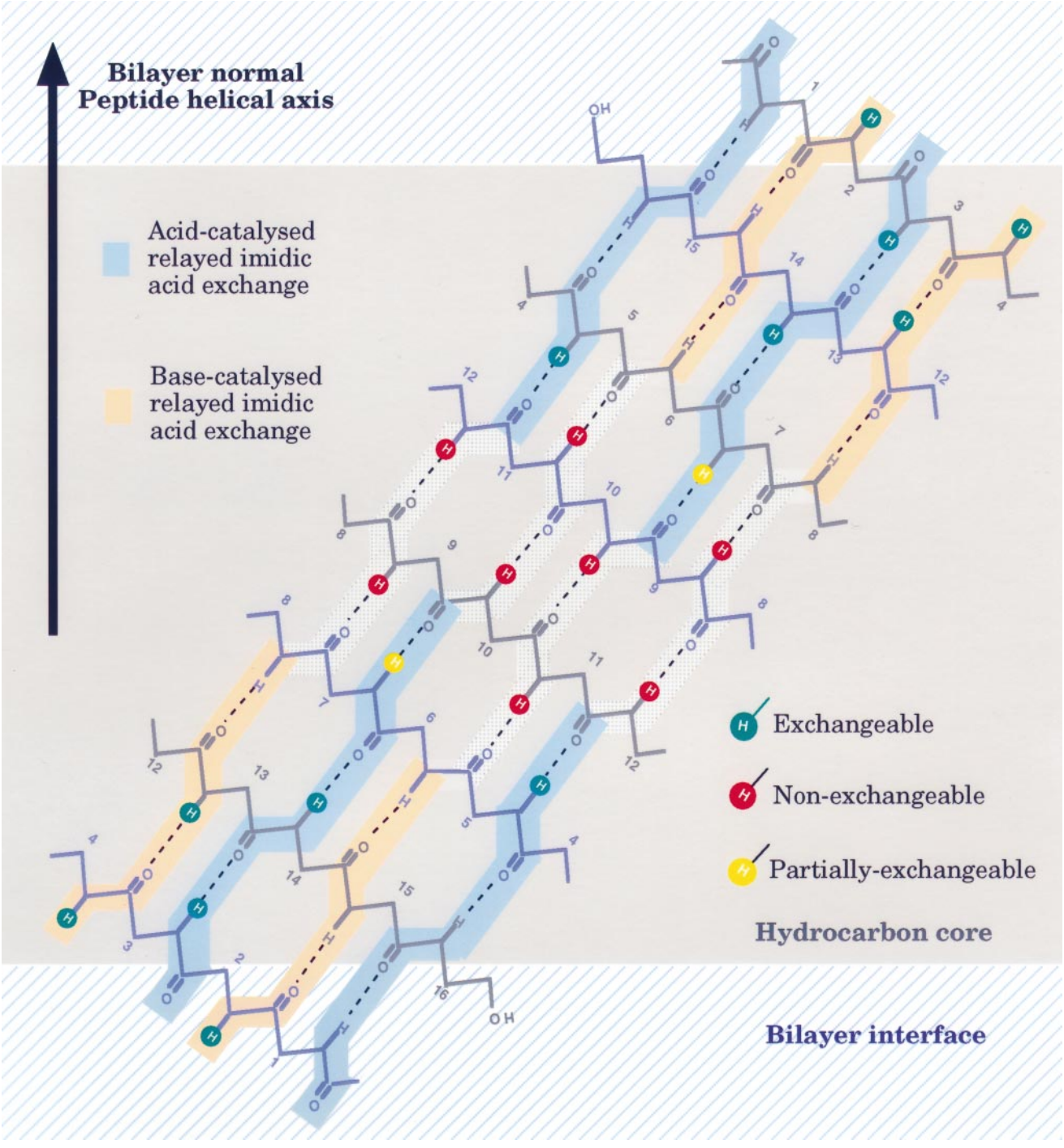

FIGURE 8 A representation of the axial projection of the hydrogen bonds in the antiparallel double-stranded gM structure represented in Fig. 1. As in Fig. 1, the two monomers are distinguished by gray and blue, but are displayed here as peptide fragments to show the hydrogen-bonding pattern. The axial or *z* coordinates of the atoms along the bilayer normal are the same as in Fig. 1; however, the *x* and *y* coordinates in the plane parallel to the bilayer surface have been modified so that the β-helix hydrogen-bonding pattern could be easily seen. The hydrophobic core (*tan*), and interface regions (*striped blue*) of the bilayer have been added using dimensions derived from Wiener and White, 1992. The acid (*blue*) and base (*orange*) catalyzed relayed mechanisms follow specific pathways. Only half of the amide protons are accessible to an acid-catalyzed relayed imidic acid exchange mechanism. The other half is potentially catalyzed by a base-catalyzed relay mechanism.

similar at the level of specific side chain conformations (Busath et al., 1998). Therefore, the conducting states observed for gM are either very rare events (conformers below detection levels by NMR) or they are nonequilibrium or metastable states. Similar rare events have been noted in other hydrophobic gA analogs (Fonseca et al., 1992). Metastable states of gA and gM have been characterized (Arumugam et al., 1996; Cotten et al., 1997). The addition of gM

as a monomer to DPhPC/decane bilayers suggests that the formation of channel states (two monomers head to head) may be a metastable state on the pathway to the equilibrium double-stranded state, which is shown here to be stable at 45°C for weeks. Consequently, there is no evidence that this species 3 structure conducts cations in a lipid environment.

While we have discussed the results of hydrogen-deuterium exchange qualitatively it is also possible to look at the results from a perspective of exchange mechanisms. Of interest is whether or not the helix is fraying at its ends to allow exchange to take place with bulk solvent or whether there is a relayed mechanism with solvent in the pore. Acid or base catalysis requires the penetration of H_3O^+ or OH^- to the site of exchange. In a hydrophobic environment this penetration is unlikely; furthermore, if this structure were to fray, i.e., the hydrogen bonds were to unzip, why then doesn't the Phe_{11} N-H exchange when the Ala_5 N-H exchanges and Val_7 N-H at least partially exchanges (Fig. 8)?

If the monomer-monomer hydrogen bonds involving Ala_5 N-H and Val_7 N-H exchange, then the hydrogen bond to Phe_{11} N-H should also break, exposing the amide proton. Such a site in a low dielectric environment must be hydrogen-bonded, if not to gM, then to the solvent, and hence the potential for exchange. Therefore, fraying does not explain the lack of exchange at the Phe_{11} N-H site. A relay mechanism which is dependent only on the penetration of water and not on the penetration of hydroxide and hydronium ions is supported by these data, as it was in the gA channel structure (Huo et al., 1996). An acid-catalyzed relayed imidic acid exchange mechanism has been extensively discussed in the literature (Eriksson et al., 1995), but a base-catalyzed relayed imidic acid exchange mechanism is also possible (Fig. 9). The acid-catalyzed version protonates exposed carbonyls (Perrin and Arrhenius, 1982) while the base-catalyzed version deprotonates the amide nitrogen. Along the potential relay pathways (highlighted in Fig. 8) there is evidence for both base- and acid-catalyzed relay mechanisms. Importantly, for base catalysis, Phe_{13} N-H exchanges while Phe_{11} N-H does not. For acid catalysis Ala_3, Ala_5, Val_7, and Leu_{14} N-H's at least partially exchange, while Leu_{10} and Leu_{12} N-H's do not. These results suggest that the acid-catalyzed relay mechanism is more effective than the base-catalyzed version. There are at least two reasons for this: even when the bulk solvent pH is approximately neutral, as it is here, the pH at the bilayer surface in the vicinity of the gM-exposed carbonyl oxygens is anticipated to be low due to the influence of the surface potential (Jordan, 1984). Moreover, the stability of a negative charge in the pore is likely to be much more difficult to achieve than stabilizing a positive charge. As a result, the acid-catalyzed relay mechanism is more effective than the base-catalyzed mechanism. This explains the lack of exchange for Phe_{11} (base-catalyzed relay mechanism) while Ala_5 and Val_7 (acid-catalyzed relay mechanism) at least partially exchange. Such local electrostatic effects occurring in the vicinity of molecular surfaces have been connected to the enhancement of acid-catalysis of polylysine by NaCl (Kim and Baldwin, 1982), Leu-Val-Ile-NH_2 peptide (O'Neil and Sykes, 1989), and M13 coat protein in SDS micelles (Henry and Sykes, 1990). In this latter example, the presence of negatively charged detergent induces the condensation of counterions, including the catalytic H^+, at their surface, thereby enhancing acid-catalysis. Overall, this exchange study of gM is an ideal situation for the relayed imidic acid exchange mechanism based on four factors suggested by Eriksson et al. (1995), i.e., 1) a hydrogen-bonding pattern allowing for the formation of imidic intermediates; 2) buried hydrogen-bonded carbonyls along the chain having low-solvent exposure; 3) dependence of the effectiveness of the exchange on the distance between the exposed carbonyl oxygens and the amide protons; and 4) the free carbonyl group at the chain extremity readily solvent-accessible.

Even with the relay mechanisms this does not rule out the possibility of some slight fraying or "natural breathing" of the structure. In fact, some deformation of the structure is necessary to allow water to penetrate at least to the level of the Val_7 N-H. The magnitude of this deformation may be

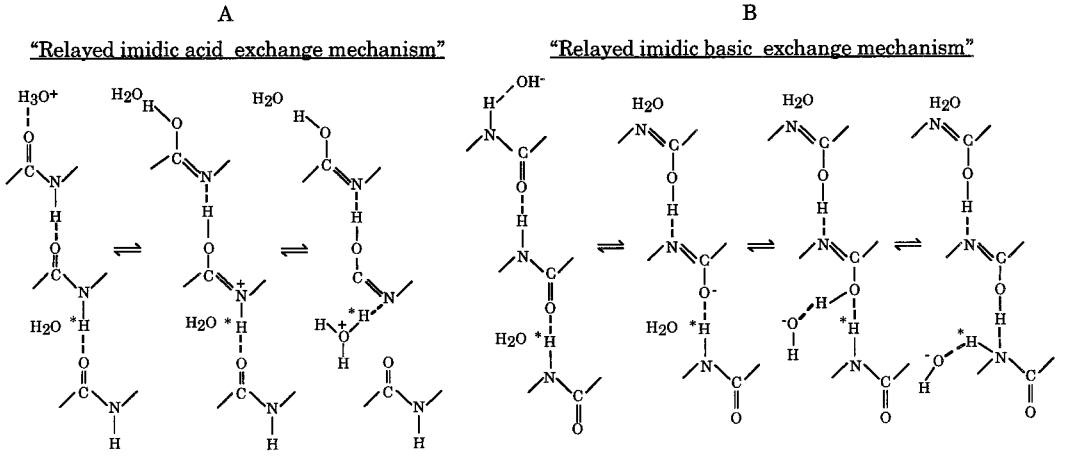

FIGURE 9 Relayed imidic acid hydrogen-deuterium exchange mechanisms. (*A*) acid-catalyzed, (*B*) base-catalyzed.

slight and may not include the breaking of peptide-peptide hydrogen bonds. Perrin (1994) argued against the relay mechanism partly because of the need to stabilize a charge and partly because of the imidic acid intermediate, which he has characterized as unstable. It should be recognized that the backbone has significant partial charges appropriate for temporarily stabilizing a hydroxide or a hydronium ion. Since those partial negative charges are larger, the acid-catalyzed mechanism would have greater probability. Overall, these data provide strong evidence for the acid-catalyzed relayed imidic acid exchange mechanism and limited evidence for the base-catalyzed version.

CONCLUSIONS

The folding motif for gM as a left-handed antiparallel double-stranded helix has been experimentally verified by solid-state NMR using both orientational and distance constraints. Such a combination of structural constraints generates a powerful structural approach and the pulse sequence SFAM has permitted the characterization of a distance from a very small dipolar interaction. Neither has such a small dipolar interaction been observed previously for characterizing a distance. Moreover, these structural constraints have been supplemented with extensive hydrogen-deuterium exchange data for the polypeptide backbone. The pathway for insertion of gM into lipid bilayers is now shown to proceed by insertion of the intact double helix without structural rearrangements that would expose the amide protons to an exchanging solvent. The exchange data also strongly suggest that this double-stranded structure does not permit the conductance of cations. Finally, two mechanisms are propagated for the exchange of the amide protons, both utilizing relayed imidic mechanisms, one acid-catalyzed and one base-catalyzed. Unique support for both of these mechanisms in bilayer solubilized gM has been presented.

The authors are indebted to the staff of the FSU National High Magnetic Field Laboratory and NMR Facilities, T. Gedris, R. Rosanske, J. Vaughn, and A. Blue, for their skillful maintenance and service of the NMR spectrometers, and H. Hendricks and U. Goli of the Bioanalytical Synthesis and Services Facility for their expertise and maintenance of the ABI 430A peptide synthesizer and HPLC equipment.

This work has been supported by National Institutes of Health Grant AI-23007 and the work was largely performed at the National High Magnetic Field Laboratory supported by the National Science Foundation Cooperative Agreement DMR-9527035 and the State of Florida.

REFERENCES

Abdul-Manan, N., and J. F. Hinton. 1994. Conformational states of gramicidin A along the pathway to the formation of channels in model membranes determined by 2D NMR and circular dichroism spectroscopy. *Biochemistry.* 33:6773–6783.

Arseniev, A. S., I. L. Barsukov, and V. F. Bystrov. 1986. Conformation of gramicidin A in solution and micelles: two dimensional ^{1}H NMR study. *Chem. Pep. Proteins.* 3:127–158.

Arumugam, S., S. Pascal, C. L. North, W. Hu, K. C. Lee, M. Cotten, R. R. Ketchem, F. Xu, M. Brenneman, F. Kovacs, F. Tian, A. Wang, S. Huo, and T. A. Cross. 1996. Conformational trapping in a membrane environment: a regulatory mechanism for protein activity? *Proc. Natl. Acad. Sci. USA.* 93:5872–5876.

Bai, Y., J. S. Milne, L. Mayne, and S. W. Englander. 1993. Primary structure effects on peptide group hydrogen exchange. *Proteins: Struct., Funct., Genet.* 17:75–86.

Busath, D., C. D. Thulin, R. W. Hendershot, L. Revell Phillips, P. Maughan, C. D. Cole, N. C. Bingham, S. Morrison, L. C. Baird, R. J. Hendershot, M. Cotten, and T. A. Cross. 1998. Non-contact dipole effects on channel permeation. I. Experiments with (5F-indole) Trp-13 gramicidin A channels. *Biophys. J.* 76:000–000.

Cotten, M., X. Feng, and T. A. Cross. 1997. Protein stability and conformational rearrangements in lipid bilayers: linear gramicidin, a model system. *Biophys. J.* 73:614–623.

Englander, S. W., N. W. Downer, and H. Teitelbaum. 1972. Hydrogen exchange. *Annu. Rev. Biochem.* 41:903–924.

Englander, S. W., and N. R. Kallenbach. 1984. Hydrogen exchange and structural dynamics of proteins and nucleic acids. *Q. Rev. Biophys.* 16:521–655.

Eriksson, M. A. L., T. Härd, and L. Nilsson. 1995. On the pH dependence of amide proton exchange rates in proteins. *Biophys. J.* 69:329–339.

Fields, C. G., G. B. Fields, R. L. Noble, and T. A. Cross. 1989. Solid phase peptide synthesis of ^{15}N-gramicidins A, B, and C and high performance liquid chromatographic purification. *Int. J. Pept. Protein Res.* 33: 298–303.

Fields, G. B., C. G. Fields, J. Petefish, H. E. Van Wart, and T. A. Cross. 1988. Solid phase peptide synthesis and solid state NMR spectroscopy of [Ala_3-^{15}N][Val_1] gramicidin A. *Proc. Natl. Acad. Sci USA.* 85: 1384–1388.

Fonseca, V. P., P. Daumas, L. Ranjalahy-Rasoloarijao, F. Heitz, R. Lazaro, Y. Trudelle, and O. S. Andersen. 1992. Gramicidin channels that have no tryptophan residues. *Biochemistry.* 31:5340–5350.

Fu, R., S. A. Smith, and G. Bodenhausen. 1997. Recoupling of heteronuclear dipolar interactions in solid state magic-angle spinning NMR by simultaneous frequency and amplitude modulation. *Chem. Phys. Lett.* 272:361–369.

Heitz, F., G. Gavach, G. Spach, and Y. Trudelle. 1986. Analysis of the ion transfer through the channel of 9,11,13,15-phenylalanine gramicidin A. *Biophys. Chem.* 24:143–148.

Henry, G. D., and B. D. Sykes. 1990. Hydrogen exchange kinetics in a membrane protein determined by 15N NMR spectroscopy: use of the inept experiment to follow individual amides in detergent-solubilized M13 coat protein. *Biochemistry.* 29:6303–6313.

Huo, S., S. Arumugam, and T. A. Cross. 1996. Hydrogen exchange in the lipid bilayer-bound gramicidin channel. *Solid state NMR.* 7:177–183.

Jordan, P. 1984. The total electrostatic potential in a gramicidin channel. *J. Mol. Biol.* 78:91–102.

Kayalar, C. 1979. A model for proton translocation in biomembranes based on keto-enol shifts in hydrogen bonded peptide groups. *J. Membr. Biol.* 45:37–42.

Ketchem, R., W. Hu, and T. Cross. 1993. High-resolution conformation of gramicidin A in a lipid bilayer by solid state NMR. *Science.* 261: 1457–1460.

Ketchem, R. R., K. C. Lee, S. Huo, and T. A. Cross. 1996. Macromolecular structural elucidation with solid-state NMR-derived orientational constraints. *J. Biomol. NMR.* 8:1–14.

Kim, P. S., and R. L. Baldwin. 1982. Influence of charge on rate of amide proton exchange. *Biochemistry.* 21:1–5.

Koeppe, R. E., and O. S. Andersen. 1996. Engineering the gramicidin channel. *Annu. Rev. Biophys. Biomol. Struct.* 2:231–258.

Langs, D. A. 1988. Three-dimensional structure at 0.86 Å of the uncomplexed form of the transmembrane ion channel peptide gramicidin A. *Science.* 241:188–191.

Langs, D. A., G. D. Smith, C. Courseille, G. Precigoux, and M. Hospital. 1991. Monoclinic uncomplexed double-stranded, antiparallel, left-handed beta 5.6-helix (increases decreases beta 5.6) structure of gramicidin A: alternate patterns of helical association and deformation. *Proc. Natl. Acad. Sci. USA.* 88:5345–5349.

Lee, K.-C., W. Hu, and T. A. Cross. 1993. ^{2}H NMR determination of the global correlation time of gramicidin channel in a lipid bilayer. *Biophys. J.* 65:1162–1167.

Linderstrøm-Lang, K. 1955. Deuterium exchange between peptides and water. *Chem. Soc. Spec. Publ.* 2:1–20.

Nicholson, L. K., and T. A. Cross. 1989. Gramicidin cation channel: an experimental determination of the right-handed helix sense and verification of β-type hydrogen bonding. *Biochemistry*. 28:9379–9385.

North, C. L., and T. A. Cross. 1995. Correlations between function and dynamics: time scale coincidence for ion translocation and molecular dynamics in the gramicidin channel backbone. *Biochemistry*. 34: 5883–5895.

O'Connell, A. M., R. E. Koeppe II, and O. S. Andersen. 1990. Kinetics of gramicidin channel formation in lipid bilayers: transmembrane monomer association. *Science.* 250:1256–1259.

O'Neil, J. D., and B. D. Sykes. 1989. NMR studies of the influence of dodecyl sulfate on the amide nitrogen exchange kinetics of a micelle solubilized hydrophobic peptide. *Biochemistry.* 28:699–707.

Pascal, S. M., and T. A. Cross. 1992. Structure of an isolated gramicidin A double helical species by high-resolution nuclear magnetic resonance. *J. Mol. Biol.* 226:1101–1109.

Pascal, S. M., and T. A. Cross. 1993. High-resolution structure and dynamic implications for a double-helical gramicidin A conformer. *J. Biomol. NMR.* 3:495–513.

Pascal, S. M., and T. A. Cross. 1994. Polypeptide conformational space: dynamics by solution NMR, disorder by x-ray crystallography. *J. Mol. Biol.* 241:431–439.

Perrin, C. L. 1994. Symmetries of hydrogen bonds in solution. *Science.* 266:1665–1668.

Perrin, C. L., and G. M. L. Arrhenius. 1982. Mechanisms of acid-catalyzed proton exchange in N-methyl amides. *J. Am. Chem. Soc.* 104: 6693–6696.

Rohl, C. A., and R. L. Baldwin. 1994. Exchange kinetics of individual protons in ^{15}N-labeled helical peptides measured by isotope-edited NMR. *Biochemistry.* 33:7760–7767.

Salom, D., M. C. Bañó, L. Braco, and C. Abad. 1995. HPLC demonstration than an all Trp→Phe replacement in gramicidin A results in a conformational rearrangement from β-helical monomer to double-stranded dimer in model membranes. *Biochem. Biophys. Res. Commun.* 209: 466–473.

Smith, S. A., T. O. Levante, B. H. Meier, and R. R. Ernst. 1994. Computer stimulations in magnetic resonance. An object oriented job approach. *J. Magn. Reson. A.* 106:75–105.

Tian, F., and T. A. Cross. 1999. Cation transport: an example of structural based selectivity. *J. Mol. Biol.* (in press).

Tian, F., K.-C. Lee, W. Hu, and T. A. Cross. 1996. Monovalent cation transport: lack of structural deformation upon cation binding. *Biochemistry.* 35:11959–11966.

Tüchsen, E., and C. Woodward. 1985. Mechanism of surface peptide proton exchange in bovine pancreatic trypsin inhibitor. Salts effects and O-protonation. *J. Mol. Biol.* 185:421–430.

Wagner, G. 1983. Characterization of the distribution of internal motions in the basic pancreatic trypsin inhibitor using a large number of internal NMR probes. *Q. Rev. Biophys.* 16:1.

Wagner, G., and K. Wüthrich. 1982. Amide proton exchange and surface conformation of the basic pancreatic trypsin inhibitor in solution. *J. Mol. Biol.* 160:343–361.

Wallace, B. A., and K. Ravikumar. 1988. The gramicidin pore: crystal structure of a cesium complex. *Science.* 241:182–187.

Wiener, M. C., and S. H. White. 1992. Structure of a fluid dioleoylphosphatidylcholine bilayer determined by joint refinement of x-ray and neutron diffraction data. III. Complete structure. *Biophys. J.* 61: 437–447.

Woodward, C., I. Simon, and E. Tüchsen. 1982. Hydrogen exchange and the dynamic structure of proteins. *Mol. Cell. Biochem.* 48:135–160.

Xu, F., A. Wang, J. B. Vaughn, and T. A. Cross. 1996. A catalytic role for protic solvents in conformational interconversion. *J. Am. Chem. Soc.* 118:9176–9177.

Zhang, Z., S. M. Pascal, and T. A. Cross. 1992. A conformational rearrangement in gramicidin A: from a double-stranded left-handed to a single-stranded right-handed helix. *Biochemistry.* 31:8822–8828.